ELSEVIER

Polymer 42 (2001) 5037–5045

polymer

www.elsevier.nl/locate/polymer

Multiple melting behavior of poly(butylene-2,6-naphthalate)

Ming-Yih Ju, Feng-Chih Chang*

Institute of Applied Chemistry, National Chiao Tung University, Hsinchu, Taiwan, ROC

Received 18 September 2000; accepted 14 November 2000

Abstract

Multiple melting behaviors of poly(butylene-2,6-naphthalate) (PBN) prepared by various crystallization conditions were studied by differential scanning calorimetry at a heating rate of 10°C/min. It is found that the crystallization rate of PBN is so rapid that the glass transition temperature cannot be detected by simply heating the quenched sample. Two melting peaks are generally perceptible in a heating scan for isothermally crystallized samples that can be properly explained by the model proposed by Zhou and Clough (Polym Engng Sci 28 (1988) 65). The low-temperature melting peak can be ascribed to the melting of primary and secondary crystals generated during the crystallization or annealing process, while the high-temperature melting peak comes from the significant contribution of the melting of recrystallized species formed during heating. The step-crystallization was performed to clarify the relationship between the melting behavior and crystal modifications of PBN. In this study, it is found that the melting behavior of PBN is independent of the crystal forms and dominated by the crystal lamellar thickness and the perfection of crystals, which are dependent upon the thermal history. Finally, an equilibrium melting temperature of 276°C is obtained for the neat PBN, which is lower than that published in the literature.

Keywords: Poly(butylene-2,6-naphthalate); Multiple melting; Crystallization

1. Introduction

The multiple melting behavior of most semicrystalline polymers has been observed for decades and been investigated extensively. There have been numerous reports on the multiple melting behaviors of poly(ethylene-2,6-naphthalate) (PEN) [1,2], poly(butylene terephthalate) (PBT) [3,4], poly(ether ether ketone) (PEEK) [5], syndiotactic polystyrene (s-PS) [6], and others. The origin of the multiple melting endotherms in certain semicrystalline polymers has been found to arise due to a variety of reasons, including (i) the presence of alternate crystal modifications, (ii) the melting of distributions of a single morphological form differing in size and perfection, and (iii) melting, recrystallization and remelting processes during the heating scan in the calorimeter. In general, it is believed that the multiple melting behavior of most of the polyesters is governed mainly by the third mechanism mentioned above.

Cheng and Wunderlich [1] reported the detailed thermal properties of PEN, such as the heat capacities in liquid and solid states and the equilibrium melting parameters, using differential scanning calorimetry (DSC). Later, Buchner et al. [2] investigated the crystallization and melting behavior of PEN via DSC and synchrotron radiation. They found that the melting behavior of PEN is independent of crystal modifications and possibly depends upon the crystal lamellar thickness, which is dominated by the selected crystallization temperature (T_c). Medellin-Rodriguez et al. [7] studied the melting behavior of three semirigid polymers, poly(ethylene terephthalate) (PET), PEN and PEEK, and proposed that the melting process is morphologically the reverse of the isothermal crystallization process with respect to primary and secondary structural elements. Recently, Sauer et al. [8] utilized a temperature-modulated DSC (TMDSC) to characterize the melting and recrystallization phenomena of PEN and obtained the results similar to those reported by Medellin-Rodriguez et al. [7]. Three melting endothermic peaks were observed, and the peaks arranging from low to high temperatures can be ascribed to the melting of the secondary and primary crystals and the recrystallized species formed during heating, respectively.

Poly(butylene-2,6-naphthalate) (PBN) is a semicrystalline polyester possessing a molecular structure similar to PEN but contains a tetramethylene segment instead of the ethylene segment in PEN:

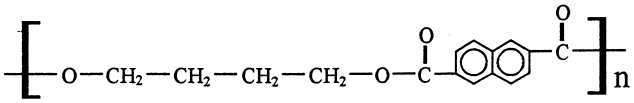

* Corresponding author. Tel.: +886-35-712-121 ext. 56552; fax: +886-35-723-764.

E-mail address: changfc@cc.nctu.edu.tw (F.-C. Chang).

0032-3861/01/$ - see front matter
PII: S0032-3861(00)00888-0

While the multiple melting behavior of PEN has been well recognized, the complete melting endotherms of PBN have not yet been studied systematically until recently. Yoon et al. [9] have studied the thermal properties and miscibility of PEN/PBN blends. Furthermore, Lee et al. [10] studied the crystallization kinetics of PBN and poly (ethylene-*co*-butylene-2,6-naphthalate) (PEBN) copolyesters, and an equilibrium melting temperature (T_m^0) of 294°C for the neat PBN was reported. Papageorgiou and Karayannidis [11] studied the multiple melting behavior of PEN, PBN and eight random PEBN copolyesters of different compositions by DSC and found that two to three melting peaks can be resolved in the thermograms of the isothermally crystallized samples, depending on the crystallization temperature. In the present work, we intend to study the multiple melting behavior of the neat PBN prepared by several different crystallization procedures.

2. Experimental

2.1. Material and sample preparation

Additive-free PBN, with an inherent viscosity of 0.62, was kindly provided by the Shinkong Synthetic Fibers Inc., Taiwan. The mass loss is less than 5% at 300°C for 180 min under nitrogen atmosphere, measured by a thermogravimetric analyzer from Perkin–Elmer, TGA-7. Before proceeding with the experiments, the PBN pellets were cryogenically crashed into fine particles (~0.1 mm) in a small type blender. Crystallization procedures were carried out in both the melt and solid state, nonisothermally and isothermally. For the nonisothermal crystallization, the PBN was heated and maintained at 280°C for 10 min, then cooled down to 25°C at various cooling rates. For the isothermal-melt crystallization, PBN was preheated at 280°C for 10 min, cooled down to the predetermined temperature at a rate of 100°C/min, maintained isothermally for the desired duration, followed by quenching in liquid nitrogen to terminate the crystallization process. In addition, stepwise melt-crystallizations were also conducted between 200 and 220°C. For the cold-crystallization, the liquid-nitrogen-quenched sample (from 280°C for 10 min) was annealed at a predetermined temperature for 3 h in the solid state, followed by quenching in liquid nitrogen to terminate the crystallization process. The detailed conditions will be described in Section 3. All of the crystallization and annealing processes were performed in the cell of the differential scanning calorimeter, and therefore the temperature can be controlled accurately (±0.1°C).

2.2. Apparatus

A DSC instrument from DuPont (DSC 2010) equipped with a liquid-nitrogen-cooling accessory was used to conduct various crystallization conditions and to detect the melting endothermic peaks. A nitrogen-purge flow at 25 ml/min was used throughout the whole experiment. A two-point temperature calibration was performed with indium and tin standards by heating at 10°C/min, and the cell constant was calibrated by indium standard. The sample weight of 10 ± 1 mg was used herein, and a constant heating rate of 10°C/min was employed from 10 to 300°C for the determination of the melting points unless otherwise indicated. The thermal properties of the samples prepared by various crystallization conditions in the melting transition region were obtained by the TA Instruments Universal Analysis software, and the multiple melting endotherms were decomposed in Gaussian with linear baseline to calculate the individual area percentage under melting peaks.

The wide-angle X-ray diffraction (WAXD) pattern of the thermally treated PBN sample in the powder form was obtained at ambient conditions using the Mac Science 18 kW rotating anode X-ray generator (M18XHF) with CuKα radiation (50 kV, 200 mA, $\lambda = 1.5405$ Å). The incident light was monochromatized by a Gr(111) crystal to eliminate CuKβ contamination. The scattering angle was measured from 5 to 40° with a scanning rate of 2°/min.

3. Results and discussion

3.1. Melting behavior of the nonisothermally crystallized PBN

The onset and peak temperatures of the crystallization exotherms in the cooling scans as a function of cooling rate are plotted in Fig. 1. Single crystallization exotherm was observed during cooling, and the position and magnitude of the exotherm are dependent on the cooling rate. At

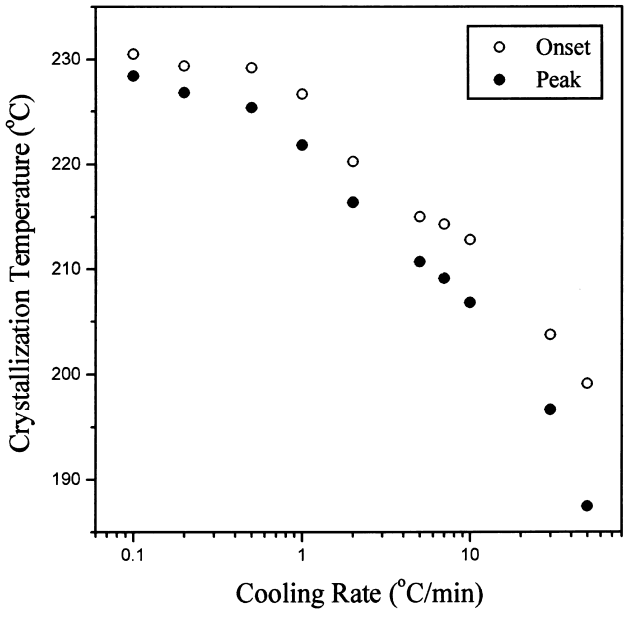

Fig. 1. Plots of cooling rate versus the onset and peak temperatures of crystallization exotherms in the cooling scans.

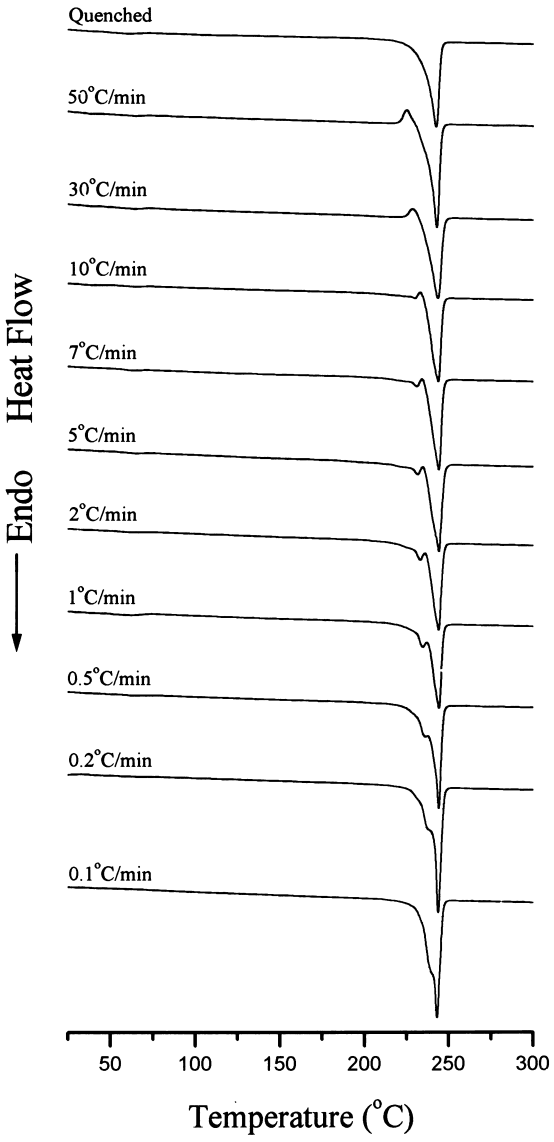

Fig. 2. DSC thermograms obtained at the heating rate of 10°C/min for the nonisothermally crystallized PBN samples prepared by different cooling rates.

the highest cooling rate, i.e. 50°C/min, the PBN exhibits the lowest exotherm temperature and has the greatest breadth between the onset and the peak temperatures. When the cooling rate is decreased, the crystallization process occurs at a higher temperature and the breadth of the exotherm is reduced as would be expected. The DSC heating thermograms of these nonisothermally crystallized PBN samples obtained by heating at 10°C/min are given in Fig. 2. Only one melting endothermic peak at 242.5°C is discerned for the quenched PBN, revealing the very rapid crystallization rate of the PBN. Actually, an opaque sample of PBN was always generated after quenching from the melt, an indication of the presence of crystalline entities. It has been reported that the crystallization rate of PBN is faster than that of PBT [12], and the half-time of crystallization for PBN decreases monotonously with T_c [13]. In general, the crystallizable molecules of most semicrystalline polymers can be retained in the random state by quenching from the melt, so the glass transition temperature (T_g) and the exotherm that resulted from cold crystallization can be observed during the heating scan. The thermogram of the quenched PBN (Fig. 2) shows neither T_g nor cold crystallization exotherm, and this result has obviously originated from the rapid crystallization rate. In fact, several different T_g values for the neat PBN have been reported in the literature [10,11,13–16] within the range of 41–82°C, due to the difficulty in obtaining the totally amorphous specimen. For the sample cooled at 50°C/min (Fig. 2), a small exotherm appears right in front of the main melting endotherm, suggesting that recrystallization occurs to form more perfect crystals. As the cooling rate is further decreased, the area of the recrystallization exotherm is reduced. A minor melting peak emerges at lower temperature (229.9°C) when the conducted cooling rate is 10°C/min or lower. This minor melting peak shifts towards high temperature and increases in size with the decrease of cooling rate, and eventually merges with the main melting peak as a shoulder on the low-temperature side (237.7°C) when the cooling rate is decreased to 0.2°C/min and lower. It is noteworthy here that the peak temperature of the main melting endotherm remains nearly unchanged (243.6 ± 0.5°C) regardless of the cooling rate. In addition, the recrystallization peak does not appear in the quenched sample compared with those prepared by high cooling rates. Although the recrystallization exotherm is absent in the thermogram of the quenched sample, it still does not imply that the recrystallization does not occur. The recrystallization process may take place during the whole heating scan for the quenched sample, so only the single melting peak is observed as the result.

3.2. Melting behavior of the isothermally crystallized PBN

A DSC heating scan on a semicrystalline polymer prepared with certain crystallization condition contains many nonequilibrium effects, including the amount of reversible melting due to the metastability of crystal morphologies in most polymers [17]. Although it has been reported that triple melting peaks are expected in many polyesters [1,7,8,11,18,19], however, double melting peaks are more generally observed in the heating scan because the melting of primary crystals is usually difficult to be detected. The triple melting behavior is explained by the model proposed by Zhou and Clough [18] who investigated the melting behaviors of the isothermally crystallized PET. This model is related to the morphological development that has been studied by optical microscopy [7] and temperature scanning small angle X-ray scattering (SAXS) [19]. In this model, early melting of secondary crystals is responsible for the low endothermic region, melting of primary crystals causes the middle endotherm, and the final endotherm is ascribed to the significant contribution from the melting of

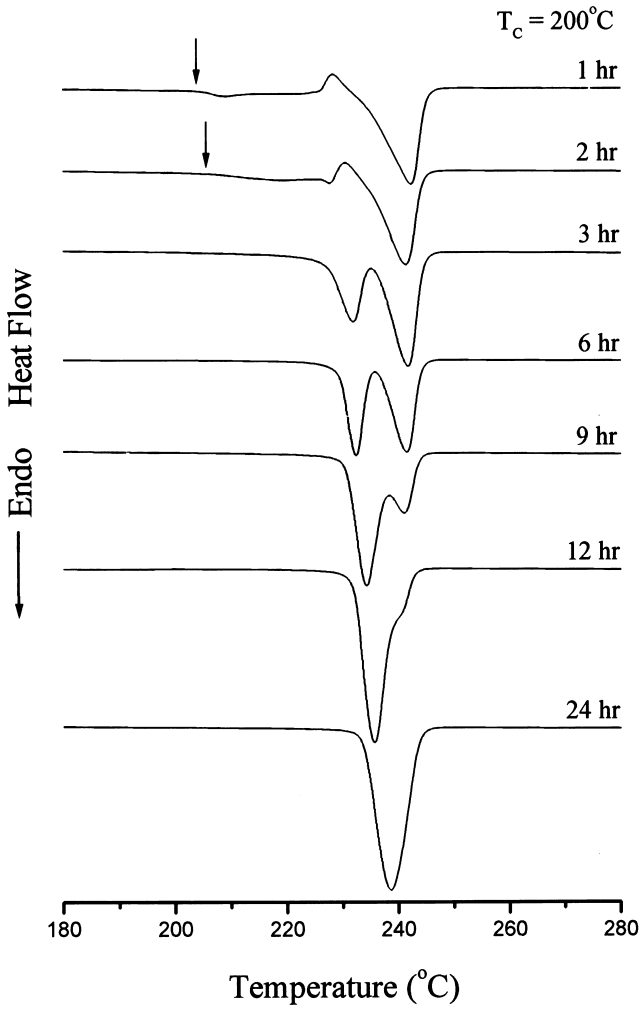

Fig. 3. DSC thermograms obtained at the heating rate of 10°C/min for the PBN samples crystallized isothermally at 200°C for different durations from the melt.

recrystallized species formed during heating. However, due to the complexity of DSC data, the expected middle endotherm resulting from the melting of primary crystals may merge with the final endotherm [20] or overlaps with the broad recrystallization exotherm. Consequently, a typical melting sequence usually observed in a heating thermogram is firstly the appearance of a small endothermic region, followed by a recrystallization exotherm, and finally a main endotherm. The final endotherm mostly comes from the melting of the recrystallized species that contributes to the majority of total heat of fusion.

DSC thermograms of the PBN crystallized isothermally at 200°C for different durations from the melt are presented in Fig. 3, where the melting behavior influenced by crystallization time is clearly demonstrated. For the sample crystallized for 1 h, the melting process begins at 203.6°C as indicated by the arrow in Fig. 3, which is only slightly higher than the T_c. Subsequently, a broad and relatively weak endotherm region appears, followed by an exotherm that comes from the recrystallization. Apparently, this endothermic region has originated from the melting of secondary crystals and perhaps from a portion of primary crystals since this region occupies a broad temperature range. As the crystallization time is increased to 2 h, the melting process begins at a higher temperature than that crystallized for 1 h, and a low-temperature melting peak (T_m^L) clearly emerges at 227.6°C. This low-temperature melting peak shifts towards higher temperature and increases in size with increasing crystallization time, and eventually a dual melting is evolved. On the other hand, the high-temperature melting peak (T_m^H), resulting from the melting of the recrystallized species, remains nearly unchanged but its size decreases with the increase of crystallization time. This result reveals that a larger fraction of the PBN molecules can crystallize into more perfect crystals when the crystallization time is prolonged, and thus the fraction that would undergo recrystallization is reduced relatively. For the sample crystallized for 12 h, the high-temperature melting peak becomes a small shoulder at 241.0°C, and finally only one single melting peak is left in the sample crystallized for 24 h. A similar trend is also observed for the samples crystallized at a higher temperature, e.g. 220°C, as shown in Fig. 4. At a higher crystallization temperature, the recrystallization exotherm is missing, and the dual melting behavior is detected within short crystallization time. Again, a single melting peak is observed for those samples crystallized with longer time (>60 min). Interestingly, a very weak shoulder is resolved at 244.2°C, which is higher than the T_m^H, and remains at the same position within 30 min of crystallization time as designated by the dashed line in Fig. 4. The special feature of the observed single melting peak in Figs. 3 and 4 should be noted here. It is known that at higher crystallization temperature and longer duration, secondary crystals have the tendency to become equivalent to primary crystals in terms of thermal stability [7,17,19]. Consequently, both secondary and primary crystals become more thermally stable and do not go through the melting and recrystallizing process during the heating scan, resulting in one melting endotherm at a higher temperature. The thermal properties obtained from Figs. 3 and 4 are summarized in Table 1. It has been clearly demonstrated in Figs. 3 and 4 that the heat of fusion of the low-temperature melting peak increases while that of the high-temperature melting peak decreases with the increase of crystallization time. Nevertheless, the total heat of fusion, which is the summation of the endothermic area under the two peaks, increases with increasing crystallization time as shown in Table 1. The total heat of fusion increases apparently within short crystallization time and levels off when the maximum crystallinity is approaching as would be expected.

The effect of crystallization temperature on the melting behavior of the PBN is represented in Fig. 5, where PBN samples were crystallized isothermally at different temperatures for 3 h from the melt. The temperature effect on the melting behavior of PBN is equivalent to the time effect as

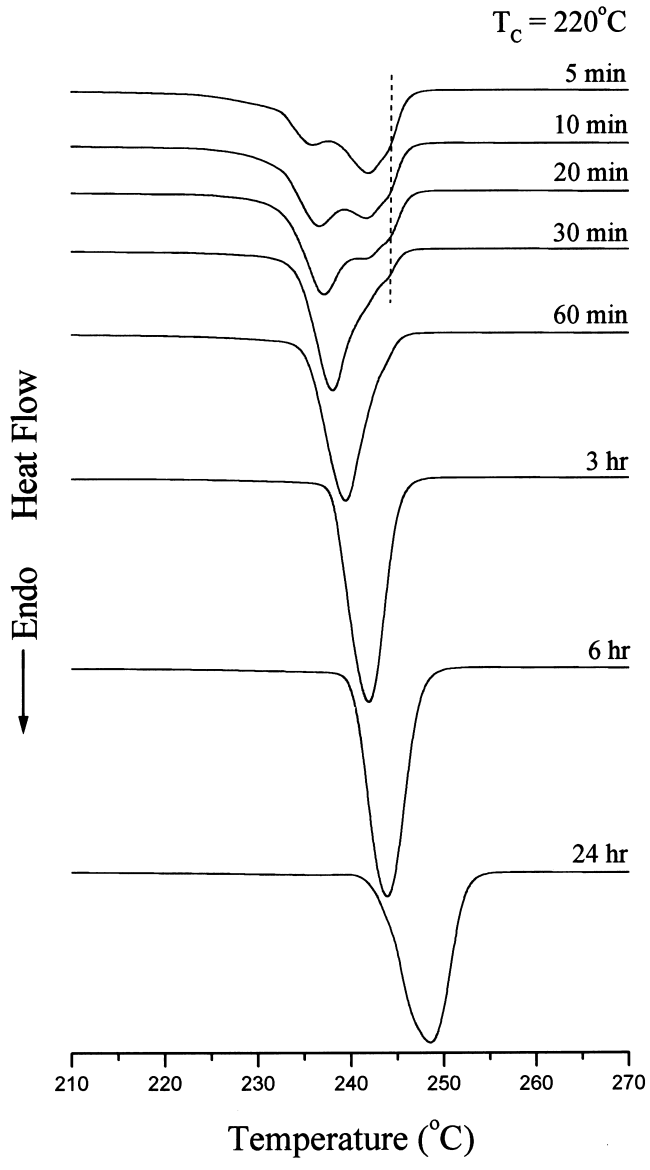

Fig. 4. DSC thermograms obtained at the heating rate of 10°C/min for the PBN samples crystallized isothermally at 220°C for different durations from the melt.

shown in Figs. 3 and 4. At a low crystallization temperature, e.g. 190°C, the recrystallization process is still significant and therefore a small exotherm is detected as shown in Fig. 5. When the crystallization temperature is increased, a dual melting is observed. Finally, only one melting peak is left when the crystallization temperature is 215°C or above. The thermal properties obtained from Fig. 5 are summarized in Table 2. Again, the total heat of fusion exhibits the trend similar to those listed in Table 1; it increases progressively with the increase of crystallization temperature.

Fig. 6 displays the DSC thermograms of the cold-crystallized PBN samples that were annealed at different temperatures in the range of 160–230°C for 3 h in the solid state. At low annealing temperatures (T_a) (<200°C), two endothermic peaks can be found in Fig. 6. A very weak melting peak appears first during the heating scan at a temperature 19–25°C higher than the T_a, followed by the main melting peak at upper temperature. Apparently, this weak melting peak originates from the melting of those less perfect crystals generated during the annealing process. This weak melting peak shifts towards high temperature with increasing T_a and eventually merges with the main melting peak. On the other hand, the main melting peak remains nearly constant at 241.6 ± 0.4°C and sharpens gradually

Table 1
Thermal properties of PBN in the melting transition region measured on heating at 10°C/min. Samples were crystallized at 200 and 220°C for different durations from the melt

T_c (°C)	Time	T_m^L (°C)[a]	T_m^H (°C)[a]	Heat of fusion (J/g)[b]		
				A_L	A_H	$A_L + A_H$
200	1 h	–	242.3	3.9[c]	30.2	34.1
	2 h	227.6	241.3	7.6[c]	29.1	36.7
	3 h	231.9	241.7	14.2	26.0	40.2
	6 h	232.4	241.5	19.0	23.7	42.7
	9 h	234.3	241.0	32.4	12.1	44.5
	12 h	235.7	241.0(sh)[d]	45.6	–	45.6
	24 h	238.6	–	45.7	–	45.7
220	5 min	236.0	242.0, 244.2(sh)[d]	13.6	20.8	34.4
	10 min	236.6	241.7, 244.2(sh)[d]	19.9	16.2	36.9
	20 min	237.2	241.5, 244.2(sh)[d]	26.5	12.1	38.6
	30 min	238.1	244.2(sh)[d]	40.4	–	40.4
	60 min	239.5	–	42.0	–	42.0
	3 h	241.9	–	44.4	–	44.4
	6 h	243.9	–	46.0	–	46.0
	24 h	248.5	–	46.2	–	46.2

[a] T_m^L, T_m^H: the peak temperature of the low- and high-temperature melting peaks, respectively.
[b] A_L, A_H: the area under the low- and high-temperature melting peaks, respectively.
[c] The small endothermic area before the recrystallization exotherm.
[d] sh: shoulder.

Table 2
Thermal properties of PBN in the melting transition region measured on heating at 10°C/min. Samples were crystallized at different temperatures for 3 h from the melt

T_c (°C)	T_m^L (°C)[a]	T_m^H (°C)[a]	Heat of fusion (J/g)[b]		
			A_L	A_H	$A_L + A_H$
190	221.6	241.9	4.9	33.9	38.8
195	227.6	241.7	7.6	31.9	39.5
200	231.9	241.7	14.2	26.0	40.2
205	235.1	241.6	26.1	14.3	40.4
210	236.6	241.7(sh)[c]	41.5	–	41.5
215	239.0	–	42.4	–	42.4
220	241.9	–	44.4	–	44.4

[a] T_m^L, T_m^H: the peak temperature of the low- and high-temperature melting peaks, respectively.
[b] A_L, A_H: the area under the low- and high-temperature melting peaks, respectively.
[c] sh: shoulder.

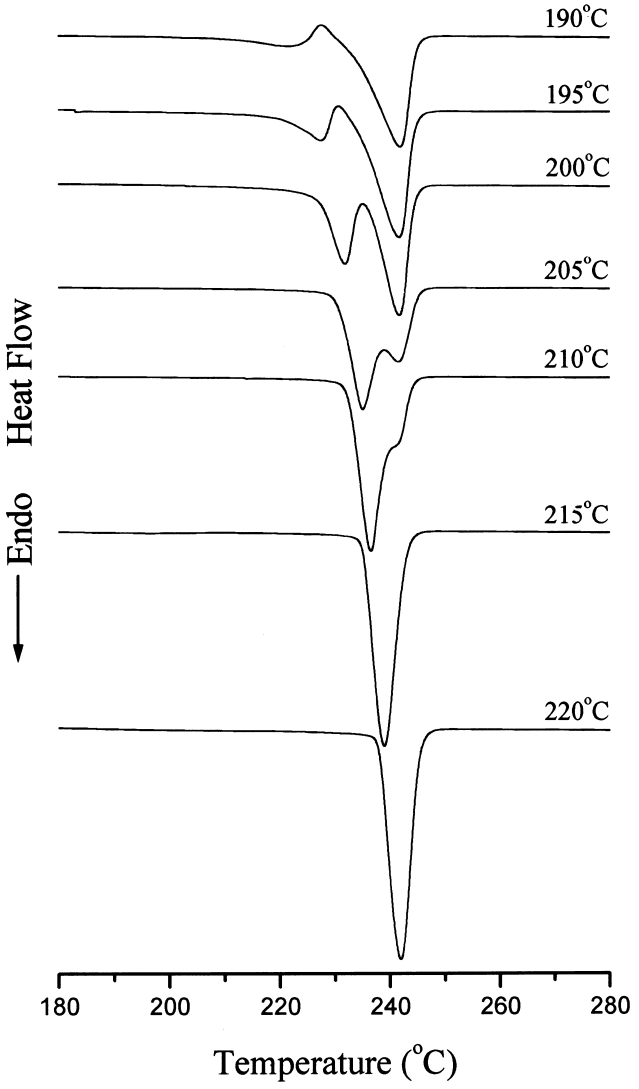

Fig. 5. DSC thermograms obtained at the heating rate of 10°C/min for the PBN samples crystallized isothermally at different temperatures for 3 h from the melt.

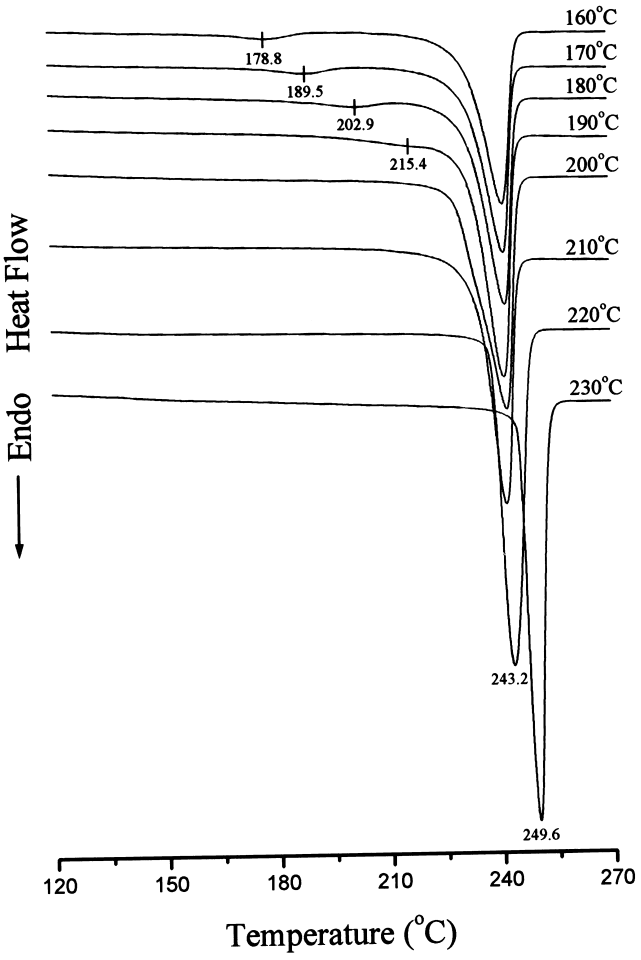

Fig. 6. DSC thermograms obtained at the heating rate of 10°C/min for the PBN samples cold-crystallized at different temperatures for 3 h in the solid state.

with the increase of T_a when the T_a is lower than 210°C. When the T_a is higher than 220°C, this main melting peak shifts to higher temperature and its shape becomes even sharper. In addition, no recrystallization exotherm is detected in all thermograms of these cold-crystallized PBN samples.

3.3. Relationship between the melting behavior and crystal modifications of PBN

It has been reported by Watanabe [21] that PBN is able to crystallize into two different crystal modifications due to the conformational change of the tetramethylene segment, which is contracted in the α form and extended in the β form. In a recent study, Chiba et al. [22] found that both α and β forms of PBN can be generated simultaneously by crystallizing the sample isothermally at 230°C from the melt under static conditions, while only the α form is obtained when PBN is melt-crystallized at 200°C. Furthermore, it is also shown that the crystalline form of PBN is determined by the initial crystallization temperature and the later annealing treatment performed at other temperature will not alter the already existed crystalline form [22]. Accordingly, in order to clarify the possible relationship between the crystal modifications and melting behavior, PBN was crystallized stepwise between 200 and 220°C in this study. Two isothermally crystallized samples were prepared at 200 and 220°C separately for 3 h using the same procedure of melt-crystallization described previously. In addition, one sample was crystallized isothermally at 200°C for 3 h from the melt, and then annealed at 220°C immediately for another 3 h by elevating the DSC temperature at 100°C/min from 200°C, followed by quenching in liquid nitrogen. This sample is designated as 200/220 hereafter. The other sample was subjected to similar procedure except that it was crystallized at 220°C first and then annealed at 200°C, and this sample is designated as 220/200 hereafter. Subsequently, the four samples prepared with different thermal

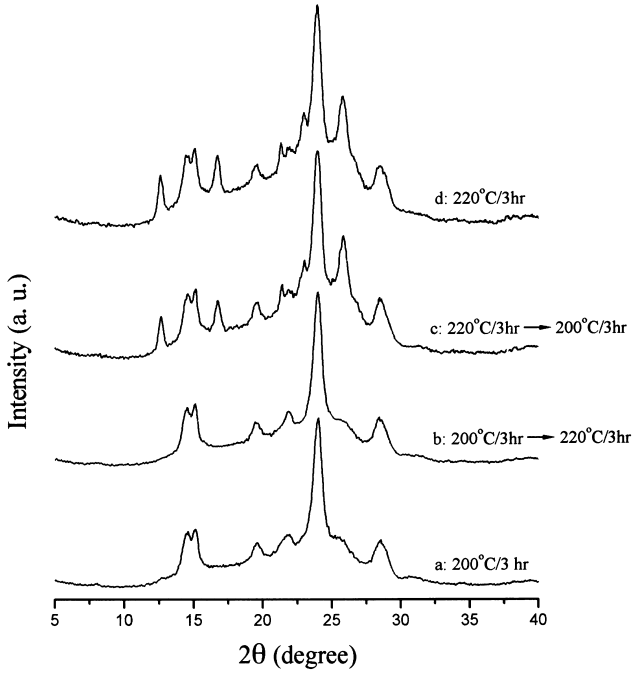

Fig. 7. WAXD patterns of the isothermally and stepwise crystallized PBN.

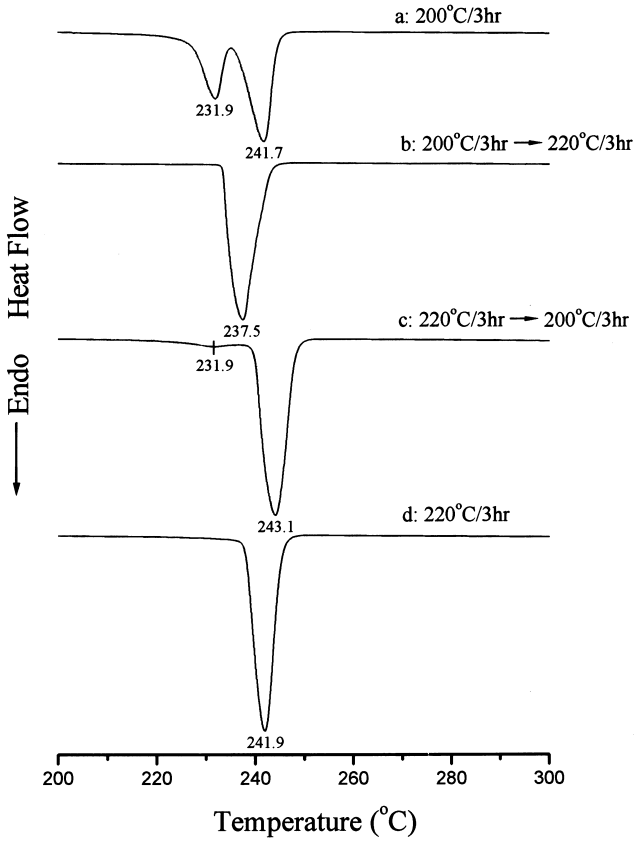

Fig. 8. DSC thermograms of the isothermally and stepwise crystallized PBN.

histories were cryogenically crushed into powder by a small type blender for WAXD examinations.

The WAXD patterns of the isothermally and stepwise crystallized PBN are presented in Fig. 7. Only the α form is detected in the sample crystallized isothermally at 200°C (Fig. 7a), while both the α and β forms are present in the sample crystallized at 220°C (Fig. 7d). These results are similar to those reported by Chiba et al. [22]. In the 200/220 sample, the α form produced at 200°C is retained as shown in Fig. 7b. The annealing process carried out at 220°C does not change the already existing crystalline form that had formed during the previous melt-crystallization process at 200°C. A similar result is also obtained for the 220/200 sample; its WAXD pattern is nearly identical to that of the sample crystallized at 220°C (Fig. 7c and d). Based on these observations in Fig. 7, the relationship between the melting behavior and crystalline forms of PBN can be examined by observing the corresponding melting behaviors of the samples prepared by the same step-crystallization procedures described above. If the crystalline form of the PBN is the only factor that influences the melting behavior, the melting behavior of the step-crystallized sample should be similar to that of the isothermally crystallized one since no change occurs in crystalline form during step-crystallization. The melting behaviors of the 200/220 and 220/200 samples as well as those crystallized isothermally at 200 and 220°C are presented in Fig. 8. The sample crystallized isothermally at 200°C for 3 h exhibits the typical dual melting behavior as shown in Fig. 8a, which has been discussed previously. However, in Fig. 8b, only one melting peak is observed at 237.5°C for the 200/220 sample. As compared with the melting behavior of the sample crystallized isothermally at 200°C for 6 h displayed in Fig. 3, the melting peak temperature of the 200/220 sample is ca. 5°C higher than that of T_m^L (232.4°C) of the one isothermally crystallized with the same total crystallization time. Furthermore, the isothermally crystallized sample exhibits double melting peaks, whereas the step-crystallized one shows only the single melting peak. By more carefully examining these two thermograms, it can be found that the melting peak of the 200/220 sample is asymmetric, which is sharper on the low-temperature side. This observation suggests that a certain contribution from the melting of those recrystallized species is still present but too weak to be detected clearly. Evidently, further annealing carried out at higher temperature (220°C) enhances the perfection of crystals, resulting in a significant reduction of the quantity of the recrystallized species. In addition, these crystals undergo the lamellae thickening during the annealing process and thus contribute to the higher melting temperature observed in the 200/220 sample. For the 220/200 sample, it is interesting to notice that two melting peaks at 231.9 and 243.1°C are present (Fig. 8c), while only one melting peak at 241.9°C is observed in the sample crystallized isothermally at 220°C for 3 h as shown in Fig. 8d. Additional information is illustrated in Fig. 9, wherein are presented the DSC thermograms of step-crystallized PBN samples that were crystallized at 220°C first for different

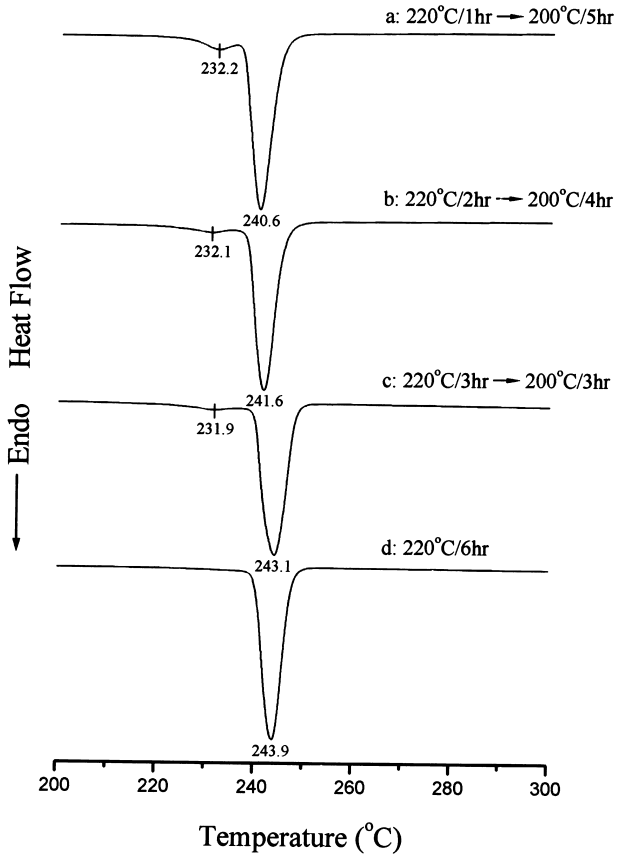

Fig. 9. DSC thermograms of the step-crystallized PBN prepared with the same total crystallization time (6 h).

durations and then annealed at 200°C to make up the total crystallization time of 6 h. Similar results are observed in these step-crystallized samples. Two melting peaks are present in the thermograms, where a weak melting endotherm manifests at lower temperature, followed by a main melting peak at upper temperature. Since it has been shown in Fig. 4 that the single melting peak can be obtained in the samples crystallized at 220°C for longer than 1 h, the main melting peak of the step-crystallized sample displayed in Fig. 9 can be attributed to the melting of the crystals generated during the initial crystallization process at 220°C. The perfection of the initially formed crystals can be further enhanced during the next annealing process that followed immediately. Consequently, the observed main melting peak temperatures for the step-crystallized samples are higher than those crystallized at 220°C isothermally with the corresponding durations. On the other hand, Table 1 shows that at $T_c = 220$°C the total heat of fusion of the sample crystallized for 1 h is lower than that crystallized for 6 h by 4 J/g, revealing the incomplete crystallization of the former sample which is able to undergo further crystallization during annealing at 200°C. Therefore, the appearance of the weak melting endotherm at 232.2°C in the thermogram of the step-crystallized sample is due to the annealing at 200°C for 5 h as shown in Fig. 9a. This weak melting endotherm decreases in size with increasing crystallization time at 220°C, which is located between 231.9 and 232.2°C that are very close to the T_m^L of the samples crystallized at 200°C for 3 and 6 h (Table 1), respectively. Consequently, the weak melting endotherm in these step-crystallized samples can be ascribed to the melting of the crystals generated during the annealing process at 200°C. According to these WAXD and DSC results, it is concluded that the melting behavior of the PBN is independent of the crystalline form and dominated by the crystal lamellar thickness and the perfection of crystals, which are dependent upon thermal histories.

3.4. Equilibrium melting temperature

The melting peak temperatures of PBN crystallized isothermally at different temperatures for 24 h from the melt are plotted as a function of crystallization temperature in Fig. 10. Two melting peaks are observed in those samples crystallized at lower temperatures (<200°C), and one single melting peak is obtained from those prepared at higher crystallization temperatures as described previously. This result is quite different from that obtained by Lee et al. [10], who observed two melting peaks until T_c is higher than 215°C. Fig. 10 shows that the position of the high-temperature melting peak is independent of crystallization temperature while that of the low-temperature melting peak increases linearly with increasing crystallization temperature. Thus, the equilibrium melting temperature of PBN can be determined by the intercept of the extrapolated T_m^L values with the line representing $T_m = T_c$ by following the Hoffmann and Weeks approach [23]. The T_m^0 of PBN thus obtained by this method is at 276°C, which is 18°C lower than that reported by Lee et al. [10] (294°C).

4. Conclusions

The multiple melting behaviors of the PBN prepared with various crystallization conditions were studied systematically by DSC at the heating rate of 10°C/min. It is found that the PBN possesses a very rapid crystallization rate and its T_g is difficult to detect by simply heating the quenched sample. The multiple melting behavior of the isothermally crystallized PBN can be explained by the model of Zhou and Clough. In general, two melting peaks are perceptible in a heating scan. The low-temperature melting peak can be ascribed to the melting of primary and secondary crystals generated in the isothermal crystallization or annealing process. The high-temperature melting peak comes from the significant contribution of the recrystallized species formed during the heating scan. The relationship between the melting behavior and crystal modifications is also clarified by performing the step-crystallization. It is found that the melting behavior of PBN is independent of the crystalline forms and dominated by the crystal lamellar thickness and the perfection of crystals, which

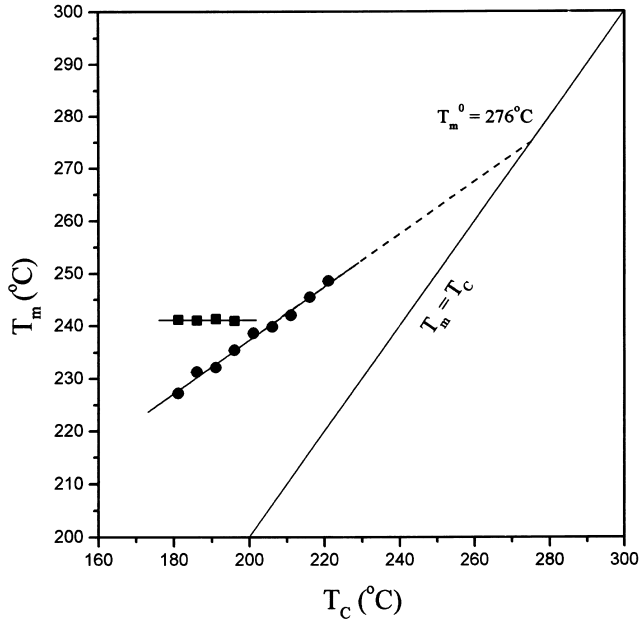

Fig. 10. Melting peak temperatures of the PBN crystallized isothermally at different temperatures for 24 h from the melt as a function of crystallization temperature.

are dependent upon the experienced thermal history. Finally, a T_m^0 of 276°C is obtained for the neat PBN in this study which is lower than that reported in the literature by 18°C.

Acknowledgements

The authors thank the Shinkong Synthetic Fibers Inc. for donation of PBN pellets and Dr Lee Hsin-Yih at Synchrotron Radiation Research Center for providing the WAXD instrument.

References

[1] Cheng SZD, Wunderlich B. Macromolecules 1988;21:789.
[2] Buchner S, Wiswe D, Zachmann HG. Polymer 1989;30:480.
[3] Yeh JT, Runt J. J Polym Sci, Part B: Polym Phys 1989;27:1543.
[4] Nichols ME, Robertson RE. J Polym Sci, Part B: Polym Phys 1992;30:305.
[5] Ko TY, Woo EM. Polymer 1996;37:1167.
[6] Lin RH, Woo EM. Polymer 2000;41:121.
[7] Medellin-Rodriguez FJ, Phillips PJ, Lin JS. Macromolecules 1996;29:7491.
[8] Sauer BB, Kampert WG, Blanchard EN, Threefoot SA, Hsiao BS. Polymer 2000;41:1099.
[9] Yoon KH, Lee SC, Park OO. Polym J 1994;26:816.
[10] Lee SC, Yoon KH, Kim JH. Polym J 1997;29:1.
[11] Papageorgiou GZ, Karayannidis GP. Polymer 1999;40:5325.
[12] Karayannidis GP, Papageorgiou GZ, Bikiaris DN, Tourasanidis EV. Polymer 1998;39:4129.
[13] Yamanobe T, Matsuda H, Imai K, Hirata A, Mori S, Komoto T. Polym J 1996;28:177.
[14] Jakeways R, Ward IM, Wilding MA, Hall IH, Desborough IJ, Pas MG. J Polym Sci: Polym Phys Ed 1975;13:799.
[15] Michaels F. Modern plastics encyclopedia. New York: McGraw-Hill, 1995.
[16] Wang CS, Sun YM. J Polym Sci, Part A: Polym Chem 1996;34:1783.
[17] Wunderlich B. Macromolecular physics, vol. 3. New York: Academic Press, 1980.
[18] Zhou C, Clough SB. Polym Engng Sci 1988;28:65.
[19] Wang ZG, Hsiao BS, Sauer BB, Kampert WG. Polymer 1999;40:4615.
[20] Qiu G, Tang ZL, Huang N-X, Gerking L. J Appl Polym Sci 1998;69:729.
[21] Watanabe H. Kobunshi Ronbunshu 1976;33:299.
[22] Chiba T, Asai S, Xu W, Sumita M. J Polym Sci: Polym Phys 1999;37:561.
[23] Hoffmann JD, Weeks JJ. J Chem Phys 1965;42:4301.